We are IntechOpen,
the world's leading publisher of
Open Access books
Built by scientists, for scientists

6,900
Open access books available

185,000
International authors and editors

200M
Downloads

154
Countries delivered to

Our authors are among the

TOP 1%
most cited scientists

12.2%
Contributors from top 500 universities

BOOK CITATION INDEX
CLARIVATE ANALYTICS
INDEXED

WEB OF SCIENCE™

Selection of our books indexed in the Book Citation Index
in Web of Science™ Core Collection (BKCI)

Interested in publishing with us?
Contact book.department@intechopen.com

Numbers displayed above are based on latest data collected.
For more information visit www.intechopen.com

Deposited Transition Metal-Centered Porphyrin and Phthalocyanine Molecules: Influence of the Substrates on the Magnetic Properties

Heike C. Herper, Barbara Brena,
Sumanta Bhandary and Biplab Sanyal

Additional information is available at the end of the chapter

Abstract

The field of molecular spintronics has gained much attention since molecules with magnetic centers form natural magnetic units, which do not suffer from the size limitations of conventional electronics, opening a new path towards miniaturization. To fabricate devices, the molecules have to be deposited on a substrate. The key questions are the interaction of the molecules with the substrate and the control of the magnetic properties. Considering molecule-substrate hybrid interfaces as building blocks for spintronic devices, a deep understanding of the electronic structure and the coupling mechanisms is central to future applications. The orientation and reconstruction of the substrates can strongly affect the electronic and magnetic characteristics of the adsorbed molecule and drastically change the properties of the free molecules. In this chapter, we will discuss the interaction of transition metal-centered porphyrins and phthalocyanines with different types of substrates, for example, ferromagnetic transition metals or graphene sheets, in the framework of state-of-the-art density functional theory methods plus insights gained from X-ray absorption/X-ray magnetic circular dichroism experiments. The goal is to give an insight into the relevant processes on the atomic scale and to present possible routes to tailor magnetic properties in molecule-substrate hybrid structures.

Keywords: magnetic molecule, density functional theory, graphene, XAS, XMCD, spin-dipole moment, spin switching

1. Introduction

Single molecular magnets play an important role in realizing the device concepts of molecular nanospintronics. In this context, spin-valves based on molecular magnets have been proposed where the exchange coupling between the magnetic center in the molecule and the magnetic electrodes dictates the magnetoresistance [1]. Among the class of molecular magnets, organometallic molecules exhibit quite complex properties due to their low dimensionality and inherent confinement effects combined with an interplay between crystal field, Coulomb interaction, spin-orbit coupling, and orbital-dependent hybridization with ligands. They exhibit enormous prospects in the context of molecular electronics/spintronics exploring the subtle balance between different energy scales. Bistability, that is, realizing two different states in the molecule which can be accessed and manipulated with external means, forms the basis of device realization. In molecular magnets, the bistability can be achieved in terms of inherent spin state or through magnetic coupling between molecule and surface while adsorbed. As will be discussed in the following sections, the choice of surface plays a crucial role in exploring both the possibilities. The subtle balance of ligand field, Coulomb energy, and Hund's exchange makes molecules with "metallic core" formed out of transition metals particularly interesting. In the molecules of our interest for this chapter, porphyrins and phthalocyanines, Fe, Co, and Mn as metal core respond to the spin crossover feasibilities. The other exotic features, for example, Kondo effect, tunable magnetic coupling, spin-orbit coupling, and orbital-dependent hybridization with ligands, also appear in this class of molecules. The description with local density approximation (LDA) within density functional theory (DFT) thus becomes inadequate and leads to a large underestimation of the highest occupied molecular orbital (HOMO)-LUMO gap. The treatment of the electron correlation hence is essential and plays an extremely significant role in determining electronic configurations, magnetic anisotropy, etc., along with the spin state. The most popular method, DFT+U, includes electron correlation in Hartree-Fock manner staying within a single particle theory where U defines the Coulomb interaction. This explicit inclusion certainly improves the situation of HOMO-LUMO gap and provides a reasonable account for spin-state, electronic configurations, and the bonding situations in the case of adsorption on different surfaces [2, 3]. The biggest advantage is to be able to simulate large systems and, therefore, is mostly used for the results we have presented here. But the method has its own limitation for finding a single Slater determinant ground state leading to the overestimation of correlation effect. A more sophisticated method has been recently adapted that includes the many-body treatment of electron correlation. This is achieved by the so-called DFT++ method, which treats an interacting Hamiltonian within Anderson's impurity model on top of the DFT Hamiltonian [4].

Although similar in structure, as shown in **Figure 1**, porphyrins and phthalocyanines behave a bit differently when adsorbed on magnetic substrates, resulting in different magnetic properties. In the examples that follow, a model system for the porphyrin molecules, that is, a porphine, is used. The porphine, a model system for the theoretical study of single-molecule magnets (SMM), maintains the same central macrocycle ring but lacks the various types of peripheral ligands that stabilize the porphyrins [5].
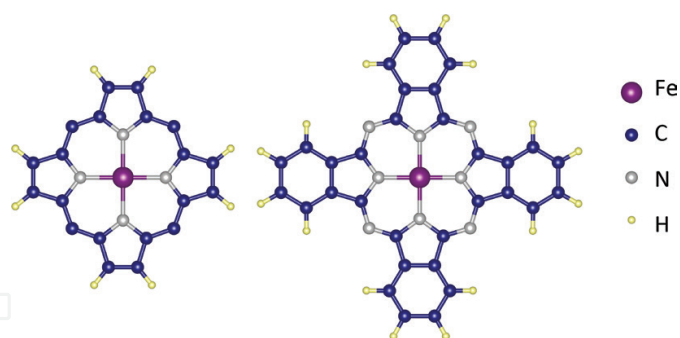
Figure 1. Porphine (left) and phthalocyanine (right) structures.

In iron porphyrin (FeP), Fe^{2+} in the center of the molecule is subjected to a square planar crystal field, along with a strong hybridization predominantly between $Fe\text{-}d_{x^2-y^2}$ and $N\text{-}p_{x/y}$ orbitals. In a strong crystal field scenario, electrons arrange themselves within the orbitals except for $d_{x^2-y^2}$ leading to an intermediate spin state, $S = 1$. However, a change in the ligand field lowers the cost of electron occupation in $d_{x^2-y^2}$ while simultaneously gains energy owing to Hund's exchange. As a result, the molecule exhibits a high spin state, $S = 2$. The energy landscapes corresponding to these two distinct spin states are however separated by an energy barrier. The estimated energy barrier within LDA+U is 0.81 eV [6]. In a square planar crystal field, structural change modifying ligand field boils down to the effective change of Fe-N bond length. In FeP, the Fe-N bond length corresponding to $S = 1$ spin state is 2.0 Å, while it needs to be stretched to 2.04 Å to achieve $S = 2$ spin state. The strain required for spin switching is however dependent on the impurity atom as well as the organic ligands. However, it is not only the gross description of spin state which should be the focus of the study. An accurate description of the electronic configuration is also required that in turns dictates crucial properties, such as magnetic anisotropy energy or spin-dipole moment. An explicit treatment of the electron correlation within many-body framework is adapted to describe the electronic structure of the molecules in addition to the DFT calculations, namely, DFT++ method. The method describes noninteracting part of the system within DFT, while an interacting Hamiltonian is treated within many-body framework, acquiring best parts of both the methods.

2. Surface effects

The deposition of molecules on suitable surfaces is an integral part of the device realization. The intrinsic gas-phase properties of molecules, however, are often diminished in that process due to structural deformation or strong chemical bonding. The focus of the chapter is to explore the feasibilities of manipulation of the molecular properties, employing surface molecular interactions yet retaining their key properties intact. Traditional electronic functions, such as memories, modulators, rectifiers, switches, transistors, and wires rely on the bistable nature associated with the charge/spin-state or molecule-surface coupling. Branching out toward spintronics, the intrinsic spin of molecules and/or magnetic coupling with a magnetic surface is exploited. In the following sections, we will explore the effects of different kinds of surfaces in controlling both the spin-state of a molecule and magnetic coupling with it.

2.1. Graphene as a reversible spin manipulator

Since the discovery in 2003, graphene has made an enormous impact on the advancement of "beyond silicon" electronics [7], as well as featuring exotic properties in multidisciplinary fields, such as gas sensing, batteries, drug delivery, understanding of high-energy experiments, and many more. We exploited its new role as an ideally ultrathin, robust 2D surface for the molecular adsorption of flat molecules like metal porphyrin (MP) or phthalocyanine (MPc) [6]. The synthesis of pristine graphene, either by exfoliation or chemical synthesis, often leaves several forms of defects on it which depending on its kind can change local structure or the whole layer structure. A "monovacancy" defect, created with a missing carbon atom, for example, has a local structural modification, while a "Stone-Wales" defect, where a much stronger reconstruction happens forming a pentagon-heptagon pair, leads to a strong ripple in the whole graphene layer. From the adsorption perspective, these distortions play crucial role and will be unveiled during the course of following discussions. However, with the present-day techniques, it is possible to create specific defects [8], which impart an access to the manipulation of molecular properties.

The adsorption of molecules or adatoms is enhanced in the presence of defects owing to the unsaturated bonds compared to that on pristine graphene with perfectly sp^2-bonded carbon network. We have investigated the adsorption scenario of FeP molecule on pristine and defected graphene. The feasibility of spin-state manipulation can be brought in only with a specific defect, "divacancy", where a pair of adjacent C atoms is missing. The binding energy of the FeP molecule on the "divacancy" site is 0.28 eV, which demonstrates its chemical stability. The molecule features almost similar structural properties as of the gas-phase molecule. However, the Fe atom experiences a vertical shift of 0.05 Å compared to that in flat gas-phase molecule. Along with that, the local defect structure modifies the square planar crystal field, experienced by the central Fe atom in the free molecule. In the electronic structure, the d_π-degeneracy which is inherent to the square planar crystal field is broken in the adsorbed molecule although the spin state remains unchanged. The schematic representation of the Fe-d orbital occupations is shown in the left part of **Figure 2**. The six electrons in Fe^{2+} ion are distributed as four and two in two different spin channel, resulting in an intermediate spin state (S = 1). The highest occupied molecular orbital (HOMO) is predominantly composed of Fe-d_z orbital, as seen in the isosurface plot in **Figure 2** (left inset). It can also be noted that the spin degeneracy is broken for the C atoms around the divacancy defect, which also contributes to the HOMO.

The surface component of the composite is exerted with a tensile strain. With as much as 1% strain, one brings sufficient change in the defect site that can affect the molecular spin state. The reconstruction in local defect structure is now prohibited with resulting stretching and unsaturated bonds, which in turn brings in sufficient mechanical strain in the molecule. The molecule switches to the high spin (S = 2) state. The crystal field, separating the $d_{x^2-y^2}$ and rest of the Fe-d orbitals, is reduced in the stretched molecule. The intra-atomic Hund's exchange overpowers the crystal filed barrier and Coulomb energy cost, and hence the spin crossover arises. The right part of **Figure 2** shows corresponding orbital occupation in the high spin state of the stretched molecule. As expected, the HOMO is now predominantly composed of Fe-$d_{x^2-y^2}$ and in-plane N-p orbitals, shown with an isosurface plot of magnetization density in the right inset of **Figure 2** [6].
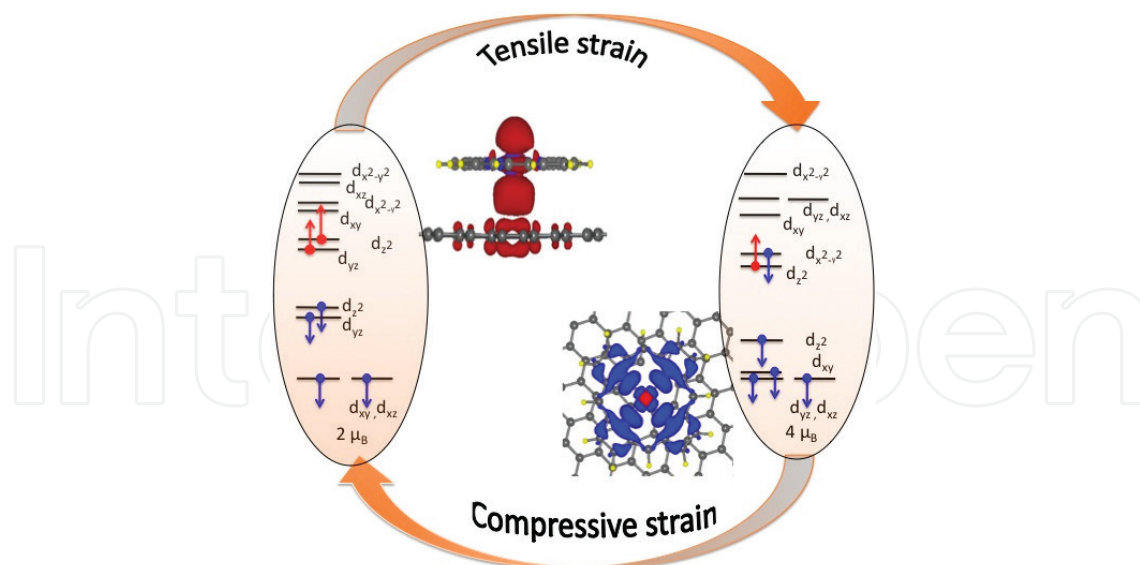
Figure 2. Magnetization density isosurfaces for FeP on (left) 0% and (right) 1% strained graphene. The isosurfaces have been plotted for an energy window of 0.4 eV below the Fermi levels in both cases. The upper (lower) plots are for spin-up (spin-down) densities. The energy levels with the d-orbital character of FeP are shown in the extreme left and right for 0 and 1% strained graphene, respectively. Data from Ref. [6].

The device realization relies on the feasibility of the controlled manipulation. This is the key achievement in this composite system. The strain engineered spin crossover is "reversible." The hysteresis effect can be brought in by applying a compressive strain (2%) to the graphene lattice. The intermediate spin state S = 1 is revived from the high spin state under compressive strain. This allows us to envisage the composite as an ultrathin spintronic device having logic states assigned as "0" and "1" corresponding to S = 1 and S = 2 spin states, respectively, which can be influenced by external strain. The strain engineered spin crossover, however, is very specific to the type of the defect in the graphene lattice and the transition metal atom in the porphyrin molecule. With a reasonable amount of strain in pristine graphene or with "monovacancy," it is not feasible to induce spin crossover in FeP.

2.2. Magnetic substrate manipulation of the spin state by chemisorption

The adsorption of iron porphyrin (FeP) on single crystal magnetic surfaces of Co and Ni shows a possible pathway to tune the molecular spin through deposition on a magnetic surface [2, 3]. The FeP molecule in the gas phase is characterized by an intermediate spin state (S = 1) [9]. In this spin configuration, the six 3d electrons of the Fe ion are distributed, four in the majority spin channel and two in the minority spin channel. A strong interaction between the molecule and the substrate can alter the electronic structure of the molecule and consequently can even affect the magnetic moment. This is even more likely to happen if the molecule adsorbs flatly, maximizing for all its constituent atoms the possibility of hybridization with the substrate. This is precisely the case of FeP on the Co and Ni substrates studied, where partially filled 3d shells can further favor a strong interfacial interaction.

DFT studies of the adsorption of FeP were performed on surfaces of different crystallographic symmetries like Ni(111) with hexagonal unit cell, Ni(110) with a rectangular unit cell, and

Ni(001) and Co(001) with square unit cells [2, 3]. The optimization of the adsorption geometries started from high-symmetry positions, like the top position, where the Fe ion is located on top of a Co or Ni atom; the bridge position, where the Fe sits in-between two metal atoms; and the hollow position where the Fe sits in-between more than two metal atoms. Different orientations of the molecule with respect to the surface major axes were also tested. In all these cases, the geometry relaxation of the hybrid interfaces resulted in short adsorption distances of about 2.0 Å or less, with a robust molecule-metal interaction indicating chemisorption. In all cases, a ferromagnetic coupling was observed. The relaxation of FeP on all these surfaces appears to be driven by the hybridization of the N atoms with the underlying Ni or Co metal atoms [2, 3]. In fact, in the case in which the morphology made it possible, the relaxations resulted in configurations where the N atoms were minimizing their distance with the Ni or Co atoms. Thus, N atoms are in many cases sitting on top positions or in proximity of a top position. To position the N atoms in this way brings about in many cases a geometrical stretching of the molecule and specifically an elongation of the intramolecular bonds between the Fe and the N atoms. The Fe-N bond lengths increased from the calculated bond length of about 1.9 Å in the gas phase [1] to values larger than 2.0 Å in the strained positions. The increase of the Fe-N bond length is directly responsible for a modification in the Fe 3d ligand field.

The different symmetries of these three substrates produce slightly different molecule-surface hybridization. On the squared (001) surfaces of both Ni and Co, FePc can arrange itself in such a way that the distances of Fe from all the four N atoms are basically the same, for example, if the Fe ion sits on the high-symmetry top or hollow sites on the surface, in these cases, the overall symmetry of the molecule is maintained (panel A in **Figure 3**), but a stretching of the bond lengths is generally observed. On the rectangular and on the hexagonal surfaces, the Fe-N bond lengths are increased asymmetrically (panels B and C in **Figure 3**). However, in all cases, a similar mechanism is observed: the elongation of the Fe-N bond lengths in FeP above about 2.04 Å causes analogous alterations of the Fe 3d crystal field, bringing about a high spin state with S = 2 on the Fe. The Fe-N bond length elongations reach up to the value of 2.13 Å
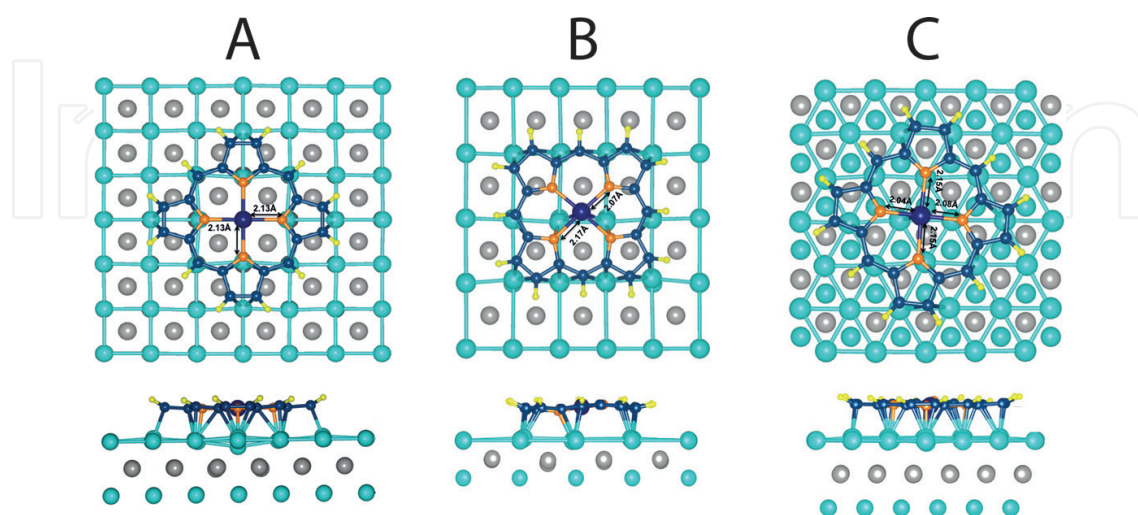

Figure 3. Top view and side view of relaxed adsorption structures for (A) FeP on Co(001), top site; (B) FeP on Ni(110), bridge site; and (C) FeP on Ni(111), hollow site. Data from Refs. [2, 3].

when adsorbed on the top site on Co(001), to values of 2.07–2.17 Å on the top site of Ni(110), to 2.04–2.15 Å on the bridge site of the Ni(111) surface. The molecular stretching corresponds a buckling of the top layer, as well as a contraction in the bond length of the underlying Co atoms in the surface layer. For example, the distance between two Co atoms beneath a FeP adsorbed on a top site on Co(001) is contracted from 2.50 to 2.44 Å.

To understand how the spin state is affected by the new strained structure of the molecule, it is necessary to look at how the electronic structure is modified by the changes in the molecular geometry. The intramolecular bonding between the N 2p levels and the Fe 3d is strictly coupled to the planar square ligand field generated by the Fe^{2+} ion, which dictates the energy separation between the 3d levels. A simple picture can illustrate how different spin states can arise in the gas phase and in the adsorbed FeP, depending on the ligand field splitting. In the gas-phase geometry, with shorter Fe-N distances, the energy splitting between the Fe 3d electrons and the N 2p electrons is such that the $d_{x^2-y^2}$ orbital remains unoccupied in both spin channels. In this case, FeP is in an intermediate spin (S = 1) configuration with four electrons in the majority and two in the minority spin channel. When the Fe-N distances are increased, the ligand field becomes weaker, leading to a smaller energy separation of the 3d states. In this case, electronic level occupation according to the Hund's rule prevails, and five orbitals in the majority spin channel and one in the minority are occupied, giving a high spin configuration (S = 2).

2.3. Magnetic coupling mechanisms between molecule and substrate

The magnetic coupling of SMM with magnetic surfaces has been studied for the iron phthalocyanine (FePc) [10, 11]. The FePc is a more stable molecule and can be easily purchased with a large variety of central atoms. Experimental studies by means of X-ray magnetic circular dichroism (XMCD) performed at HZB-BESSY II investigated the magnetic coupling between FePc and the Co(001) surfaces. The XMCD measurements were carried out at 32 and 300 K on 0.8 ML of FePc deposited first on the bare Co(001) and then on the same surface covered by an oxygen adlayer, forming a $O(\sqrt{2} \times 2\sqrt{2})R45°$ superstructure on top of the Co(001) surface. The XMCD spectra reported in **Figure 4** show how the ferromagnetic (FM) coupling of the FePc with the Co substrate is turned into antiferromagnetic (AFM) coupling in the presence of the O adlayer. The adsorption of FePc on the Co(001) surface has different characteristics with respect to the FeP.

A DFT investigation using the PBE+U method and including van der Waals corrections (D2) confirmed the FM coupling of the FePc to the Co surface. Structural relaxations starting from different high-symmetry adsorption sites, and from one nonsymmetric adsorption site, lead in all cases to chemisorption and FM coupling of the molecule on the surface. A detailed analysis of the ground state configuration (**Figure 4**) shows that the planar structure of the molecule is perturbed by a buckling, where the Fe and the N atoms directly bonded to Fe are lifted by 0.28 and 0.35 Å with respect to the metal substrate. This indicates that the C atoms in the benzene rings and the outer N atoms play a larger role in the hybridization with the surface, since they are closer to the underlying atoms. This enlightens a different adsorption mechanism in comparison to the FeP described in the previous section, where the
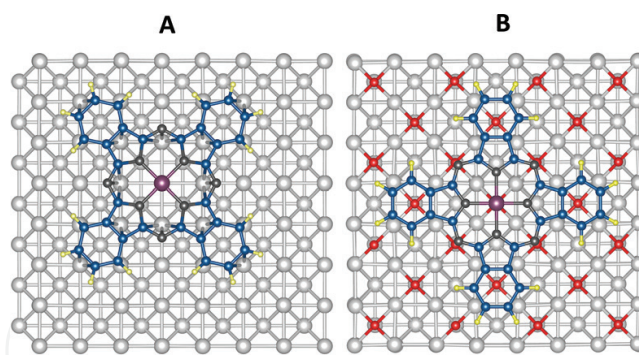
Figure 4. (A) Ground state of FePc adsorbed on Co(001) (top site). (B) Ground state of FePc adsorbed on O 2 × 2/Co(001) (top site on O atom). The dark circles indicate the O adatoms on the Co(001) surface.

hybridization with the surface mainly involved the N atoms. Moreover, the Fe-N bonding lengths are not strongly changed when the FePc are adsorbed, with calculated values of 1.97 Å in comparison to experimental values of 1.93 Å [10]. The adsorbed FePc is in the intermediate spin state (S = 1) as in the gas phase.

An important change in the magnetic structure of the hybrid interface is obtained when the Co surface is decorated by a 2 × 2 O layer. The presence of the O layer reduces the interaction of the molecules with the substrate. In fact, the magnetic coupling between the FePc and the Co substrate turns into AFM, as shown by the XMCD spectra (**Figure 5**) and also confirmed from the DFT calculations.

The lowest energy adsorption configuration obtained for the bare Co(001) and for the Oxygen plus Co is shown in **Figure 4**. It has to be observed that the relaxation of the adsorbate system formed by the molecule plus the oxidized substrate leads to different possible adsorption positions having similar energies (i.e., energies differing by less than 0.7 eV), suggesting that the molecule could in principle occupy different adsorption sites. When the O adlayer is present, the center of the FePc molecule (i.e., the Fe ion) is positioned on top of an O atom, as had been also observed for FeP on the same substrate. In this case, the distance between the Fe ion and the O atom beneath amounts to 2.19 Å, suggesting the possible formation of a chemical. The distance between the Fe and the Co atom beneath the O is 3.17 Å, indicating a weaker coupling between the Fe and the Co surfaces than was obtained for the direct adsorption on the bare Co(001). The former configuration favors an AFM superexchange coupling between the Fe(II) ion in the FePc and the underlying Co atom via the O atom in-between. An illustration of this comes from the magnetization density isosurface depicted in **Figure 6** that shows how the Fe in FePc is ferromagnetically coupled with the Co atoms while it is antiferromagnetically coupled to the same atoms in the presence of the O adlayer.

2.4. FeP on graphene/Ni(111): defect controlled magnetism

A free-standing graphene lattice with sp²-bonded C network is spin degeneracy. The creation of specific kinds of defects breaks the spin degeneracy locally, but the correlation among
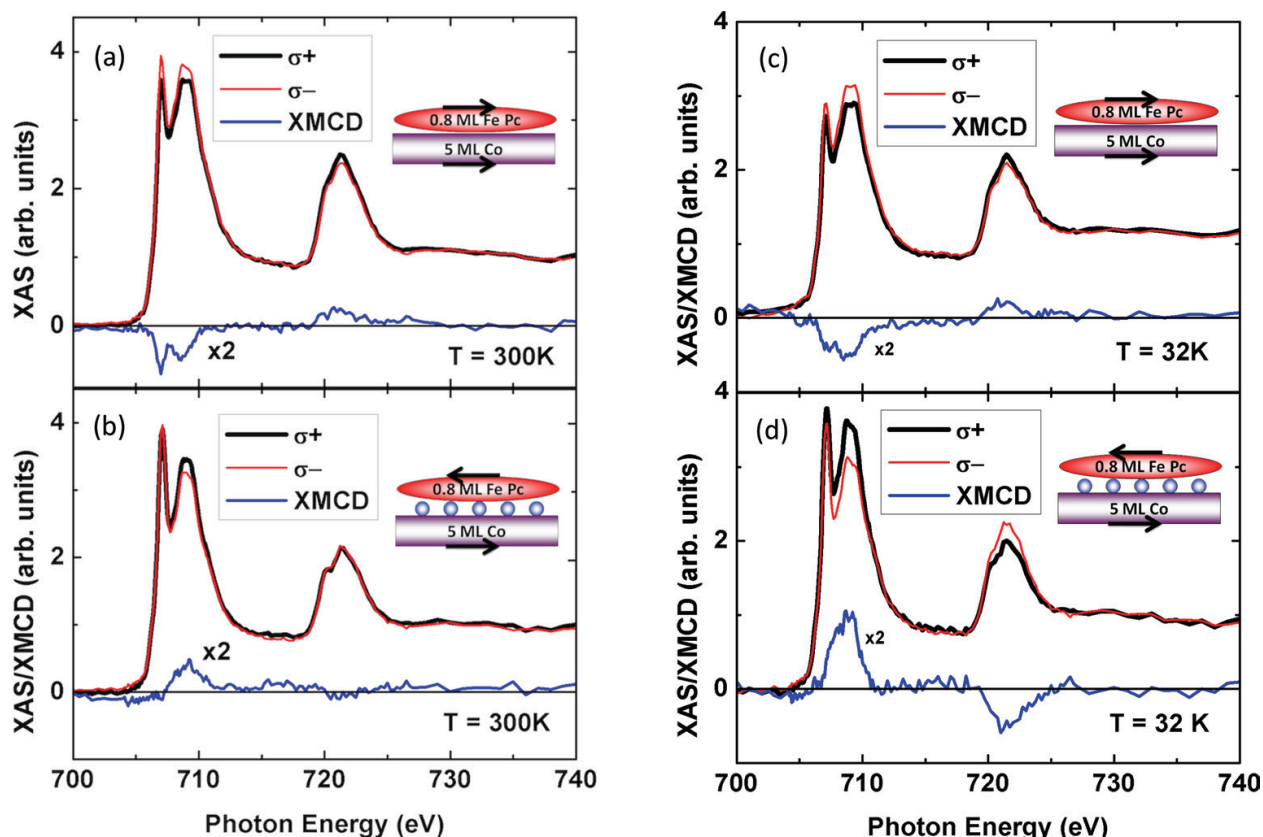
Figure 5. Fe $L_{2,3}$ XMCD spectra of 0.8 ML FePc adsorbed on (a) bare Co(001) and on (b) O/Co(001). The spectra are measured at T = 300 (left panel) and 32 K (right panel) and at a grazing angle of 70°. Data from Ref. [10].

those moments is insignificant. For the applications in the realm of molecular switch or valve, the role of graphene is inadequate albeit being extremely interesting in bringing in the spin crossover in FeP molecule. A very strong magnetic coupling and spin crossover is feasible with molecular adsorption on magnetic surface, as described in Section 2. Both the magnetic coupling and the spin state are extremely robust and are hard to manipulate. From this aspect, a composite surface, composed of a magnetic surface, such as Ni and Co and nonmagnetic "buffer" layer, fits in perfectly as it retains a magnetic coupling between the magnetic molecule and the surface but tones down the coupling strength in order to be influenced with external means. Graphene, in the presence of natural defects, appears to be an extremely potential candidate to play the crucial role of the "buffer" layer to manipulate both the spin states and magnetic coupling.

The hexagonal (111) facet of Ni surface provides an excellent platform for the deposition of the graphene layer owing to an almost perfect lattice matching. However, the unit cells of Ni(111) and graphene possess one and two atoms, respectively. In a pristine graphene layer, one of the two sub-lattice C atoms, C_A, makes direct bond with Ni atom. The bond forms out of a strong overlap between Ni-d_z and dispersive C-p_z orbitals. The other sub-lattice C atom, C_B, has much weaker overlap with Ni-d orbitals. This asymmetric hybridization has a twofold effect. Firstly, the spin degeneracy is broken and finite magnetization appears in graphene lattice. Secondly, C_A and C_B are magnetized differently.

In a pristine graphene layer on Ni, the C_A atoms acquire magnetization of 0.018 μ_B, each aligned antiparallel with respect to the Ni moments. The other sub-lattice atoms, C_B, gain relatively larger moment of 0.029 μ_B coupled ferromagnetically to the Ni moments. Altogether, the graphene layer acquires the characteristics of a ferrimagnet [12] with alternating sub-lattices having unequal opposite spin polarization, as shown in **Figure 6(a)**.

The presence of defects in graphene results in an intricate magnetization profile. The absence of C_A in a monovacancy defect does not change either structure or magnetization drastically compared to those of pristine layer. As shown in **Figure 6(b)**, sub-lattice magnetization remains the same except for the missing atom. The divacancy defect, however, has a larger impact on the local structure and hence the magnetization. A Ni atom is dragged up from the surface to heal divacancy making chemical bonds with unsaturated C bonds. The effect transmits through the graphene lattice, and the total induced moment is reduced, although the sub-lattice patterning of the magnetization remains unaltered, as presented in **Figure 6(c)**. The largest deviation from pristine graphene structure and magnetization is introduced by Stone-Wales defects. A pronounced reconstruction at the defect center creates ripple in the graphene lattice, which in turn affect graphene-Ni bonding. The corresponding magnetization profile is presented in **Figure 6(d)**. As can be seen, the alternate sub-lattice magnetization patterning at the defect site is destroyed, and effective total moment in the layer is also reduced.

The magnetic moments of the Ni atoms at the topmost layer also face the consequences of modified hybridization with C atoms at the defect sites. For a pristine graphene lattice deposited on Ni, the magnetic moments in the first Ni layer have a regular periodic pattern. The absence of C
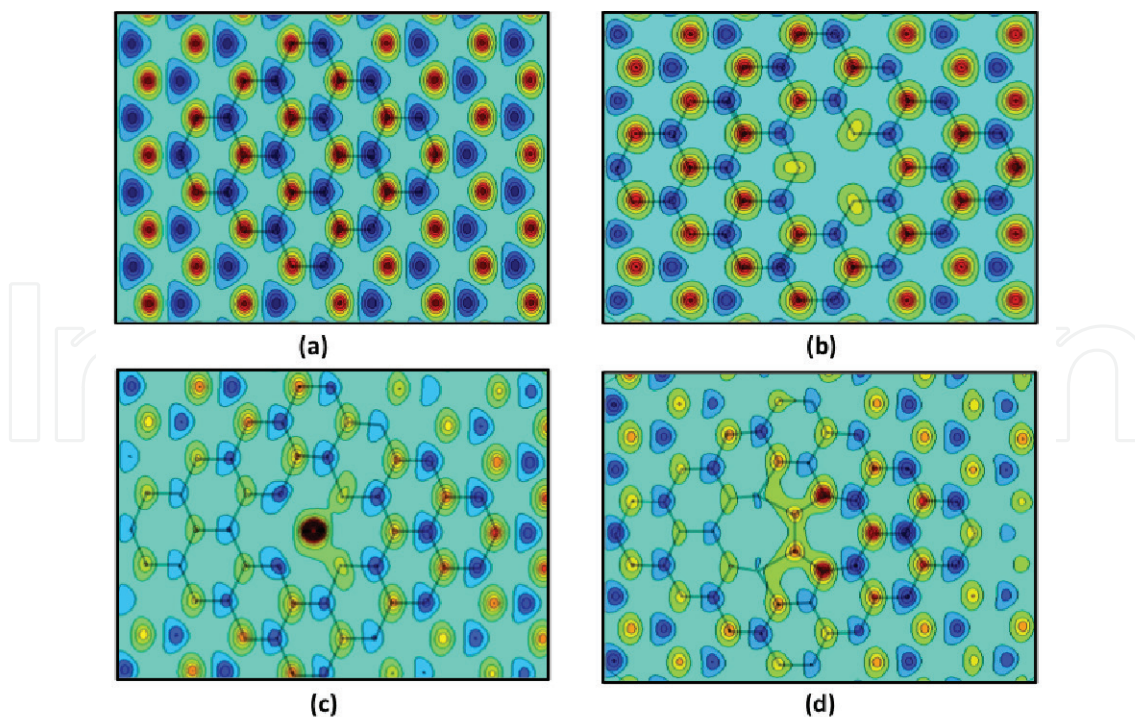

Figure 6. Magnetization densities in the graphene lattice on Ni(111) (a) without any defect, (b) with a monovacancy, (c) with a divacancy, and (d) with a SW defect. Both positive and negative densities are shown. Data from Ref. [12].

atoms in monovacancy defects reduces the coordination of Ni atoms closest to it, resulting in a larger moment. The closest Ni atom in divacancy defect comes out of Ni layer with a quenched moment. Interestingly in Stone-Wales defect, the surface Ni magnetization follows the ripple pattern. The adsorption of magnetic molecules and their properties largely depends on these combined effects at the pristine and defected sites [12].

The adsorption sites for the FeP molecule on the defect-free graphene can be identified as, Top-A, that is, on top of C_A; Top-B, that is, on top of C_B; and Hex, that is, on top of the C hexagon. The local interactions are evidently different on these three sites owing to the arrangement of molecular pyrrole ring with respect to the C atoms underneath. The induced strains in the molecule are different on these adsorption sites, and it is on the Hex position where sufficient molecular stretching occurs to realize a spin crossover. On Top-A and Top-B, molecule retains its free molecule spin state, S = 1. The average distance between the molecule and graphene is calculated to be 3.1 Å, and the graphene is 2.1 Å separated from topmost layer of Ni surface. This makes an effective separation of 5.2 Å between Fe in FeP and Ni topmost layer. On the defect-free graphene, the binding energy is highest on Hex (2.22 eV) position, but it is merely 2 and 17 meV away on Top-A and Top-B sites, respectively. The magnetic coupling is evidently much weaker than the chemisorption scenario. On the Hex site, the molecule is hardly coupled magnetically with the Ni surface. On Top-A, the exchange coupling strength is ~1.8 meV with Fe moment aligned parallel to Ni moments but antiparallel to the C_A moment (−0.018 μ_B). The alignment is quite opposite on Top-B site, where Fe moment is coupled parallel to the C_B moment (0.029 μ_B) and they both align antiparallel to the Ni moment. The coupling is also significantly strong (7 meV) compared to the other two adsorption sites.

The adsorption scenario and magnetic states of FeP are quite diverse on defect sites, depending on the local structural modifications. On the monovacancy defect, the Fe center of FeP molecule resides right in-between three C_B atoms, which have local moments aligned parallel to the Ni surface moments. The spin state of FeP resembles that of the free molecule. The molecule is coupled antiferromagnetically to the Ni surface with an exchange coupling of 7 meV. The healing of divacancy with Ni atom makes adsorption scenario strikingly different. The divacancy defect behaves like a magnetic surface, leading to chemisorption through a chemical bond formation between Fe in FeP and displaced Ni atom. The molecular pyrrole ring, however, experiences electrical repulsion form the graphene layer which imparts a convex structure to the molecule. The displacement of the Fe atom from molecular plane results in the stretching of Fe-N bond, and the molecule exhibits a high spin state (S = 2). Due to a strong orbital overlap, the magnetic coupling strength is rather high (22 meV) and is antiferromagnetic in nature. The free molecular spin state is retained on Stone-Wales defect, despite having heavily rippled graphene layer. Adsorbed FeP couples antiferromagnetically to the Ni surface. The exchange coupling is 14.5 meV which is fairly strong among all the physisorption scenarios [12].

As discussed above, the feasibility of magnetic state manipulation on this composite surface is particularly dependent on the controlled creation of specific defects. It is, hence, essential to have a quantitative estimation of the defect formation energies (DFE). In a free-standing

graphene layer, the estimated DFE for the vacancy formation is 7–8 eV, while the calculated values of DFE for monovacancy and divacancy on Ni(111) surface are 2.91 and 3.83 eV, respectively. One can safely conclude that the creation of defects, either naturally of ion-beam irradiation, should be easier in the Ni-graphene composite surface which provides a large boost for the abovementioned magnetic state manipulation. Moreover, the spin state and the magnetic coupling are adsorption site dependent; the protection of it requires a sufficient energy barriers between adsorption sites. The energy barrier in moving a FeP molecule between a Hex site and a Top-A site (which are energetically comparable adsorption sites) on a pristine graphene is calculated to be 33 meV, which translates to a temperature, higher than the room temperature. On the defect sites, this energy barrier is expected to be much higher, making the abovementioned value to be the lower limit for the diffusion barrier. One may envisage controlled formation of specific types of defects and achieving either parallel or antiparallel orientation of Fe moments relative to the moments in the Ni layers [12].

3. Nonmagnetic substrates

In the previous section, TMP or TMPc molecules deposited on magnetic substrates have been discussed in view of magnetic coupling and manipulating the spin state. In these hybrid structures, the magnetic coupling between molecules and substrate plays a dominating role. However, adsorbing molecules on nonmagnetic (NM) substrates instead allow to study aspects which are hidden in the presence of a magnetic coupling between molecule and substrates as the hybridization between molecule and substrate depending on the surface orientation and reconstruction. Thinking of future spintronic devices, the magnetic properties of the molecules can be tuned by ligands attached to the molecular center. Without the dominating magnetism of the FM substrate, only the coupling between the molecule and possible ligands exists, and this can be more easily switched by thermal treatment than the large coupling between FM and molecule.

3.1. Influence of the surface texture on the electronic structure

The electronic structure of molecules adsorbed on magnetic layers can strongly differ from the one obtained for the molecule in gas phase because of the magnetic coupling, and molecules are often chemisorbed. Here we use FeP as a model system. It corresponds to the Fe OEP structure but without the outer ethyl groups. Dangling bonds are saturated by hydrogen, see **Figure 1**.

On a nonmagnetic substrate, Cu(001) in our case, the molecules are less tightly bound to the substrate. The distance between the Fe ion of FeP and the Cu(001) substrate is about 2.66 Å (PW91, vdW-D2, U_{eff} = 3 eV) compared to 1.78 Å on Co(001), that is, the molecules are physisorbed [13]. The adsorption position and the relative orientation are the same as on the FM substrates, which means that in this system, the adsorption position is not influenced by the magnetism of the substrate but by geometry. Even though on Cu(001) there is no magnetic interaction with the molecule, the molecules hybridize with the substrate which can be seen

from the density of state (DOS) in **Figure 7(a)**. The Fe 3d states having components in z-direction (z^2 and π) are broadened compared to the DOS of the free molecule. However, the interaction is much weaker and does not lead to strong changes in the orbital occupation other than in the case of Co or Ni substrates. The Fe-N distance is basically the same as for the molecule in gas phase (2 Å) which entails that the spin state is not affected if FeP is absorbed on Cu(001), and it remains in the S = 1 state which agrees with the experimental observation from X-ray absorption spectroscopy (XAS) and X-ray magnetic circular dichroism (XMCD) [13].

The situation changes if the Cu(001) surface is covered by 0.5 layers of oxygen. This O adlayer leads to a √2×√2R45° missing row reconstruction of the surface. The ground state configuration changes from the hollow site (as on Cu(001)) to the missing row position with two O atoms next to the Fe ion. Because the O layer is basically incorporated in the surface layer of the Cu film, the distance between the Fe ion and the substrate increases only by 0.3 Å, and despite the strong surface reconstruction, the Fe-N distance increases only to 2.03 Å, that is, the spin state remains S = 1 and only minor changes in the Fe 3d DOS can be observed; see **Figure 7(b)**. Mostly the broadening of the peaks is reduced compared to the molecule on the plain Cu surface meaning that the hybridization is weaker than the Cu(001).

While the O adlayer had a huge influence on the magnetic properties when added to a ferromagnetic substrate, for example, for FePc on Co(001) or FeOEP on Co(001) [2, 3], here the spin state and the electronic structure are basically unchanged. Only the adsorption position is affected due to the surface reconstruction.

3.2. Influence of ligands

As discussed above, an O adlayer on nonmagnetic Cu(001) has no effect on the magnetic properties of the molecule, but there exist other combinations of magnetic molecules and nonmagnetic substrates where adlayers or dopants switch the spin state, for example, GaAs(001) and Vanadyl Pc. The molecule switches to the high spin state if the (Ga-rich) GaAs substrate is doped with Si. However, thinking of spintronic devices, a reliable, controllable switching
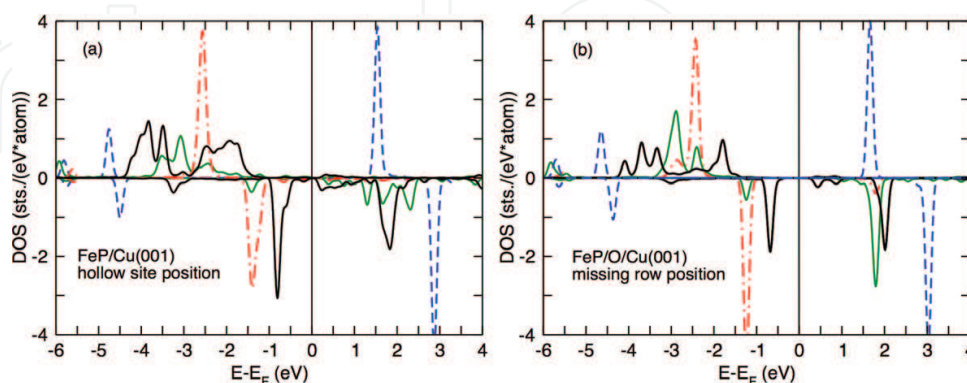

Figure 7. Calculated density of states of FeP/Cu(001) (a) and FeP/√2×v2R45°O/Cu(001) (b) for the ground state configurations with FeP on the hollow site of the Cu(001) surface with the N atoms on top of the underlying Cu atoms (a) and adsorbed on the missing row position of the reconstructed surface. Note only the Fe 3d states are shown here. Data are taken from Ref. [13].

between two configurations, for example, low spin to high spin state, is needed. This can hardly be achieved if the manipulation of the spin state arises from adlayers or doping of the substrate layer. A more realistic way is the manipulation of the spin state by ligands since ligands can be thermally attached and removed. This has been demonstrated for Co tetraethylporphyrin on Ni(001) and also works for nonmagnetic substrates. This works also on nonmagnetic substrates. Fe octaethylporphyrin (OEP) can be stabilized in air by pyridine (Py) or Cl. Depositing the two types of Fe OEP on Cu(001), they show a completely different spectroscopic signature [13], as can be seen from the X-ray absorption spectra and the X-ray magnetic circular dichroism for Fe OEP-Py and Fe OEP-Cl on Cu(001) (**Figure 8**). Especially for normal incidence, the XMCD signal is four times larger in the case of Cl ligands, whereas for grazing incidence of the photon beam, no significant differences exist; see **Figure 8**. This indicates that the magnetic and electronic properties depend on the ligand. While Py dissolves during the deposition process, that is, pure FeP remains on the substrate, in the case of Cl, about 50% of the ligand remains, which leads to an increase of the magnetic signal. Theoretical calculations for FeP (porphyrin without the outer ethyl groups) with an axial Cl ligand deposited on Cu(001) confirm the observation. The Fe-d level occupation has changed, the previously occupied d_π levels have moved above the Fermi level, and the hybridization with the substrate has decreased leading to sharper peaks compared to FeP/Cu(001). The reason is that the Fe ion also interacts strongly with the ligand.

Having seen that for a sub-monolayer coverage of Fe OEP on Cu(001) 50% of the Cl atoms which remain after deposition of the surface is sufficient to cause significant changes in the magnetic behavior, a detailed study of possible ligands and their influence on the magnetic properties has been performed for free and deposited FeP molecules [14]. In gas phase, the influence of various combinations of porphyrin or phthalocyanine and ligands (axial or peripheral) has been investigated. Here we focus on the molecule ligand complex
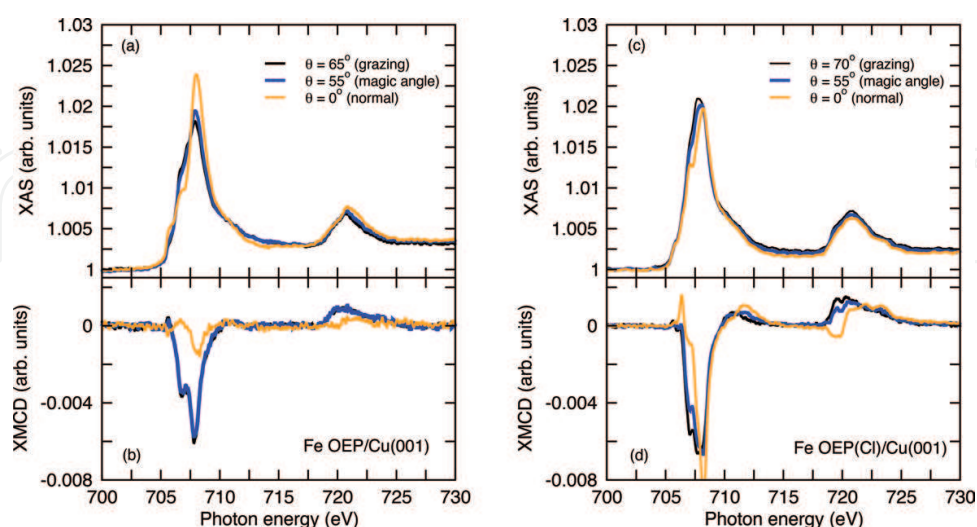

Figure 8. Measured Fe $L_{2,3}$ edge XAS (a) and XMCD (b) for 0.4 ML Fe OEP on Cu(001). Panels (c) and (d) show the analogous results for Fe OEP (Cl)/Cu(001). The angle θ denotes the angle between surface normal and photon beam. Taken from Ref. [13].

FeP+L deposited on Cu(001) with L = Cl, O,O_2. DFT calculations (VASP, PAW, PBE, and vdW-D2) show a significant dependence of the electronic and magnetic structure depending on the ligand. In all cases, the molecules have been adsorbed on the hollow site position (**Figure 9(a)**), which has been found to be the ground state for FeP/Cu(001). In agreement with the XAS/XMCD experiments described above, an axial Cl ligand enhances the magnetic moment of the FeP complex from 2 to 3 μ_B, whereby 2.69 μ_B are on the Fe ion. If the FeP-Cl complex is deposited on Cu(001), the moment becomes even larger (3.71 μ_B), and the induced moment of the Cl atom decreases from 0.2 to 0.1 μ_B. On the contrary the Fe-N distance increases from 2.05 Å for FeP/Cu(001) to 2.23 Å with Cl ligand which agrees with the observation of the transition from an intermediate spin state (S = 1) to the high spin state. The ligand has also indirect influence on the organic rings; they are driven away from the surface visible in a strong bending of the molecule; see **Figure 8**. This contrasts with FeP or FePc on magnetic substrates where also the organic ligands contribute to the interaction with the substrate.

In the case of O ligands, that is, atomic oxygen or O_2, a different magnetic behavior is observed. The spin moment on the Fe ion is reduced, while the oxygen atoms gain a moment parallel to Fe such that the spin state of the whole complex is unchanged and the total moment remains 2 μ_B. The theoretically determined spin moment of an atomic oxygen ligand is 0.58 μ_B, whereas for the oxygen dimer, the moment is evenly distributed on both O atoms (0.22 μ_B/0.21 μ_B). The latter result deviates from the gas-phase solution where the two O atoms differ in size and relative orientation. In gas phase the Fe atom has a slightly enhanced moment compensated by the antiparallel moment of the outer oxygen ligand.

Though no magnetic coupling between surface and molecule is present in the case of Cu(001), a significant interaction between substrate and molecule is observed between Fe and Cu which condenses in the change of the electronic and magnetic structure of the adsorbed molecules and is connected to severe changes in the geometrical structure. Furthermore, a deformation or buckling of the substrate next to the molecule is observed which is particularly pronounced for Cl and O ligands, while with O_2 as a ligand, the surface is much less affected. Indicating that for the dimer the interaction with the substrate is weaker than in the case of atomic Cl or O even though the adsorption distance is very similar, 2.28 Å (2.23 Å) with O_2 (O) for Cl the average distance between substrate and Fe is even larger (2.50 Å) [14].
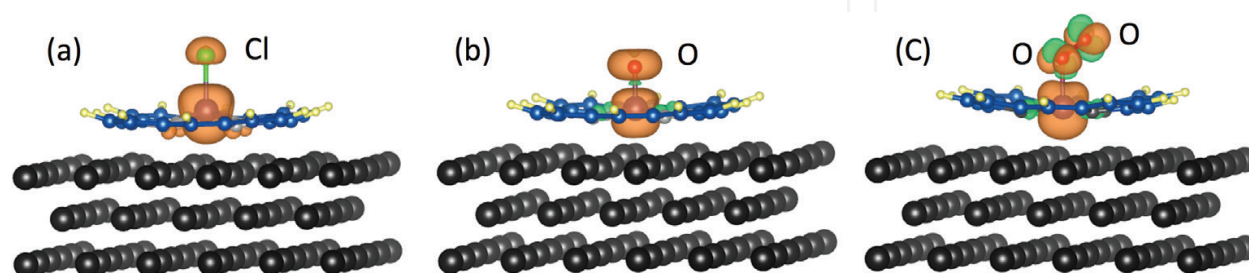

Figure 9. Calculated spin density of FeP with different axial ligands, Cl (a), atomic O (b), and O_2 (c), adsorbed on Cu (001). Both positive and negative densities are shown. Data are partially taken from Ref. [14].

In conclusion, it has been shown that the spin moment of FeP or the iron center itself can be tackled by the choice of the ligand in gas phase as well as on nonmagnetic Cu(001), whereby the changes for deposited molecules are even more expressed.

3.3. Effective spin moment and the role of the spin dipolar term

To compare the calculated spin moments with experimentally determined values, we face a problem since most experimental data are obtained from XMCD measurements. From these kinds of experiments, only orbital and effective spin moments m_{eff} are accessible. The effective spin moment differs from actual spin moment by the spin-dipole moment contribution, and depending on the symmetry, this contribution can be large [1, 10]. Comparing the XMCD signal of the Fe OEP L_3 edge (**Figure 8(c)**) for different incidence angles of the photon beam, it turns out that the intensity strongly varies with the angle. A large signal is observed for grazing incidence in much larger than for normal incidence of the photon beam. This can be caused by a large contribution of the spin-dipole term or be related to large magnetocrystalline anisotropy. Following Oguchi [16], the spin-dipole operator T is defined by

$$T = \sum_i Q^{(i)} s^{(i)} \tag{1}$$

with Q being the quadrupole tensor:

$$Q_{\alpha\beta}^{(i)} = \delta_{\alpha\beta} - 3 \, \hat{r}_{\alpha}^{(i)} \, \hat{r}_{\beta}^{(i)}. \tag{2}$$

Hence, the spin-dipole moment arises from the asperity of the spin density, that is, for transition metals where spin-orbit coupling is weak; this is related to the crystal field. If the cubic symmetry is not broken, Q vanishes, but for systems with reduced symmetry as for clusters [15, 16] or molecules adsorbed on substrates, the spin-dipole moment plays an important role [17]. To compare calculated spin moments to experimentally reported effective spin moments for low symmetry systems, the dipolar term must be included, especially to rule out other sources for the discrepancy between the effective spin moment and the total spin moment, such as a large magnetocrystalline anisotropy or not fully saturated magnetic moments. For simplicity, we focus only on the z component of the spin-dipole operator. Its expectation value $<T_z>$ is given by the trace of the density matrix multiplied by T_z. the density matrix can be obtained from DFT calculations. If for transition metals the spin-orbit coupling is negligible, the size of $<T_z>$ depends on the existence of a finite spin moment on the nonequivalent charge distribution on the orbitals. To obtain the spin-dipole moment and the effective spin moment by van der Laan [18] provided a scheme how to apply the general approach to a typical XMCD experiment such as in **Figure 10**.

The intensity which is measured in XMCD experiments as response to the photon beam hitting the surface depends on the relation between the magnetization direction **M**, the polarization of the incident photon beam **P**, and the surface normal **n** as depicted in **Figure 10**. The angular dependence of the dipole operator reads then

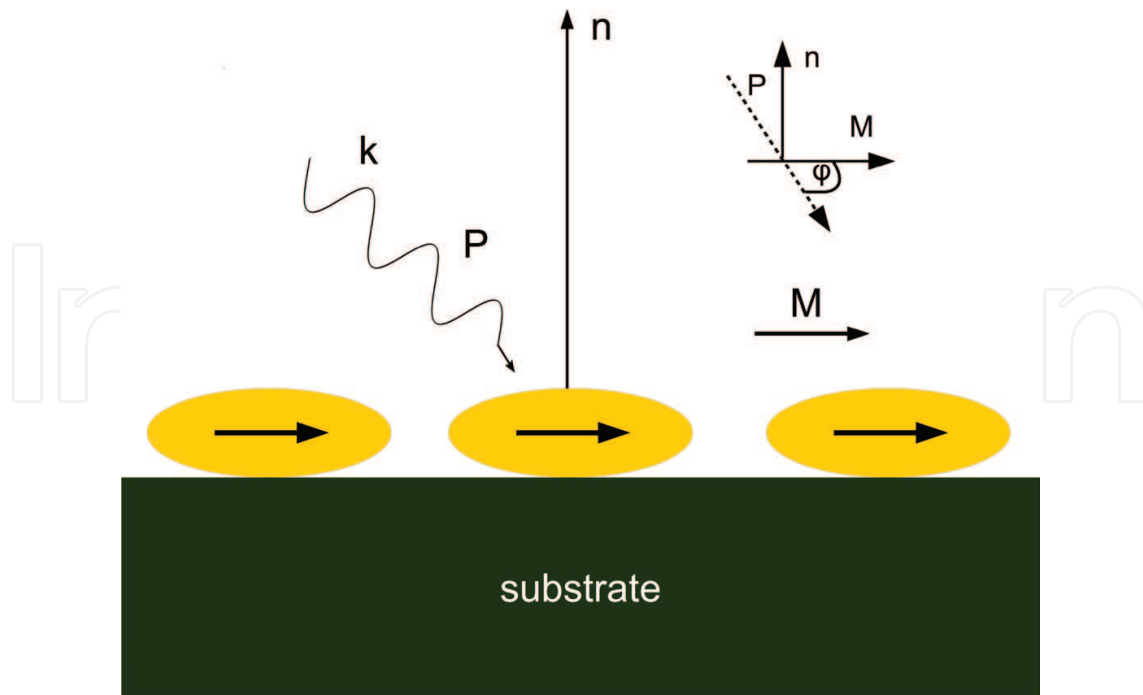$$\langle 7T\,(n, P, M)_i \rangle = \tfrac{1}{4} \langle 7 \, T_z \rangle (cos(\varphi) + 3cos(\varphi + 2\theta)) \tag{3}$$

Figure 10. Sketch of a typical experimental XMCD setup. The polarization of the photon beam and the magnetization are denoted by **P** and **M**, respectively, as well as **n** denoting the direction of the surface normal.

with φ being the angle between the magnetization **M** and the polarization of the beam **P**. The deviation of the magnetization direction from the surface normal **n** is denoted by the angle θ. In the present case, that is, for nonmagnetic substrates, the alignment of the magnetic moments of the transition metal centers of the molecules is achieved by applying an external magnetic field which is usually parallel aligned to the polarization of the incident photon beam $\mathbf{M} \| \mathbf{P}$. In this special case, Eq. (3) reduces to

$$\langle 7T(\theta)_i \rangle = \tfrac{1}{4} \langle 7\,T_z \rangle (3\cos^2(\varphi) - 1) \tag{4}$$

and the experimentally observed effective spin moment becomes

$$m_{eff} = m_s + \langle 7T(\theta) \rangle. \tag{5}$$

As can be seen from **Figure 11**, the effective moment strongly depends of the incidence angle of the photon beam. Only for measurements carried out at the *magic angle* (54.5°), the argument in the brackets on the right side of Eq. (4) vanishes, and it yields $m_{eff} = m_s$.

In an ideal case, the calculated and the measured effective moment should be identical; however, comparing the calculated m_{eff} to the experimental data (triangles) in **Figure 11(a)**, distinct deviations occur even for the magic angle where T_z vanishes. This is related to the fact the experimental sample could not be fully saturated in the magnetic field (5.9 T) [13]. For the oxidized surface, the density matrix is almost identical with the one for the plain Cu substrate; hence, also the m_{eff} and the angular dependence do not change. In this case, the theoretical and
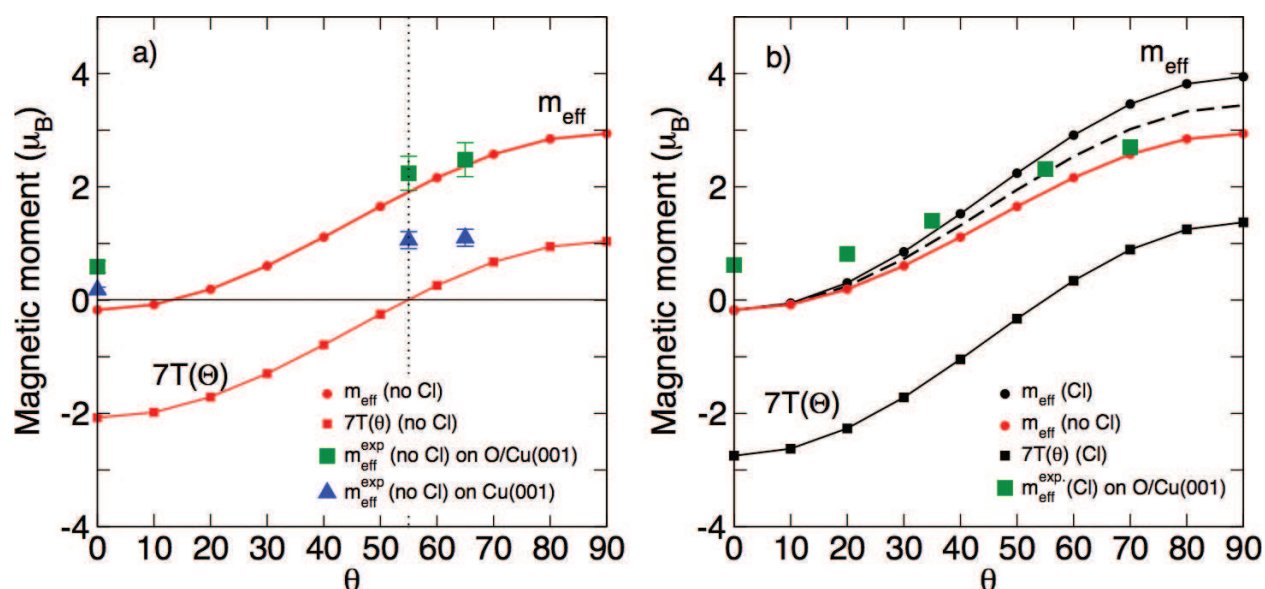
Figure 11. Dipolar term and effective spin moment for FeP on Cu(001) (a). Open (filled) symbols denote the dipolar term (effective spin moment). The data for FeP with Cl ligand are given in (b). The lighter solid line corresponds to meff without Cl, and the dashed line is the average of meff with and without Cl. Deviations between the calculated and measured m_{eff} at small incidence angles may result from limited accuracy of the determination of the dipolar term. Data are partially taken from Ref. [13].

experimental data are in good agreement, because the saturation could be reached. With a Cl ligand attached to the FeP, the dipolar term is different due to changes in the occupation of the Fe 3d levels (cf. **Figure 11**). The m_{eff} at $\theta = 90°$ would be 4 μ_B instead of 3 μ_B as without Cl. Even though the sample is basically saturated, the data deviate from the theoretically predicted spin moments. Assuming only 50% of the Cl ligands remain at the FeP molecules after deposition (dashed line in **Figure 7(b)**) improves the agreement between theory and experiment significantly. Scanning tunneling microscopy images of the Fe OEP (Cl)/Cu(001) have verified the assumption that between 40 and 60% of the ligands have been dissolved during deposition.

In summary, as shown for the example of FeP (OEP) on Cu(001), the dipolar term is an important factor to interpret and understand experimental XAS and XMCD data since effects from non-saturated samples as well as incomplete dissolved ligands can be detected.

4. Field-regulated switching of magnetic coupling

In this section, we move a step ahead to devise a practical mechanism to control magnetic bistability with external means. The composite is specifically designed with three layers of CoOEP molecules deposited on graphene-covered clean Ni(111) single crystal, as shown schematically in **Figure 12**. The focus in this composite will be on the manipulation of magnetic coupling leaving the spin crossover feasibility aside.

The CoOEP molecular layers are physisorbed on the graphene-Ni composite surface, quite resembling the FeP adsorption, discussed above. The arrangement of the molecular layers
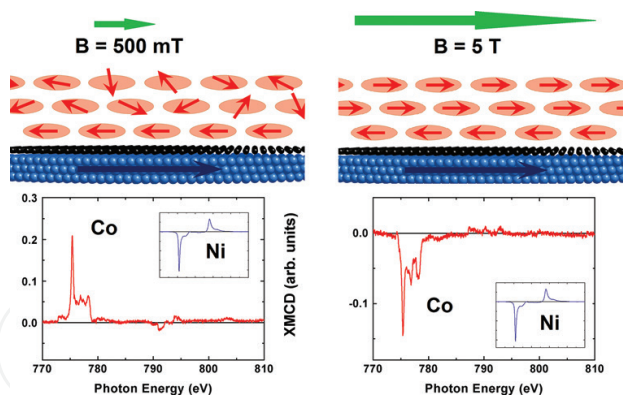
Figure 12. Top: schematic images of the sample 3ML CoOEP/graphene/Ni(111). The light and dark arrows indicate the direction of the magnetic moments of Ni and Co in a low magnetic field of 500 mT (left) and in a high magnetic field of 5 T (right). Bottom: XMCD at the Co $L_{2,3}$ edges of the CoOEP molecules in the low magnetic field (left) and in the high magnetic field (right). Insets show the XMCD at the $L_{2,3}$ edges of the saturated Ni crystal at 500 mT and at 5 T. All spectra are recorded at T = 2 K and Θ = ~70°. Data from Ref. [19].

appears in a particular fashion. The molecules in the two consecutive layers do not reside right on top of each other but slightly horizontally shifted. An indirect overlap between Co-d$_z$ orbitals via N-p orbitals favors this specific geometry. As discussed in the previous section, the single layer graphene on Ni is spin polarized with two different kinds of sub-lattice moments. Unlike FeP, in CoP the S = 1/2 spin state is quite robust and solely arises from the singly occupied Co-d$_z$ orbital, while other orbitals are doubly occupied giving no contribution to the molecular moment. However, in the presence of three layers, the net magnetization of the CoOEP molecules appears to be a sum of two contributions; the first layer couples antiferromagnetically with the Ni substrate, and the other two layers are magnetically decoupled but grow parallel magnetization with applied magnetic field. To resolve the strength of the magnetic coupling between the first CoOEP layer and Ni surface, we considered three adsorption sites in a defect-free graphene, Top-A, Top-B, and Hex, as described above. Unlike FeP, the Top-A site is energetically most favorable, while binding energies on Top-B and Hex sites are 14.6 and 23.5 meV lower. The magnetic coupling also varies in strength on these three sites exhibiting 4.2, 9.9, and 3.1 meV, respectively, on Top-A, Top-B, and Hex sites, while in all cases, molecular moments align antiferromagnetically with respect to Ni moments [19].

The CoP layers in a free-standing, perfectly parallel bilayer couple antiferromagnetically to each other. However, in practice the extended outermost ligands in CoOEP destroy the flat arrangement of the layers, reducing drastically the interlayer coupling. We modeled the scenario by increasing spatial separation and introducing angle between molecules, which essentially results in a sharp drop in the exchange coupling strength [19].

The system is then exposed under a magnetic field (B). The magnetization of the Ni layer is saturated for B > 200 mT, which is inadequate to magnetize the paramagnetic layers of CoOEP molecule. The antiferromagnetic coupling between the first layer and Ni surface requires extremely strong field to switch magnetization. The effective coupling between CoOEP layers and Ni remains antiferromagnetic under a sufficiently low field. However, as the strength of the applied field is increased, at about 1 T, the paramagnetic molecular layer grows sufficient

magnetization to revert the net orientation of the molecular magnetization parallel to the Ni magnetization. In **Figure 12**, we represent this field-induced switching of the magnetization. With an applied magnetic field as low as 500 mT, the material-specific X-ray magnetic circular dichroism (XMCD) spectra for Ni and Co show opposite orientation, as can be seen in the left part of **Figure 12**. In a sufficiently strong field, the paramagnetic layers get magnetized and overpower the antiferromagnetic contribution from the first layer. The XMCD signals for Co and Ni at 5 T are presented in the bottom-right part of **Figure 12**, which show this parallel alignment [19].

The realization of the field-regulated switching of molecular magnets is a key advancement toward molecular spintronic concepts. The spin injection into the organic layers can be regulated by an external magnetic field which may lead to the practical realization of a spin switch or spin valve in the near future.

Author details

Heike C. Herper[1], Barbara Brena[1], Sumanta Bhandary[2] and Biplab Sanyal[1]*

*Address all correspondence to: Biplab.Sanyal@physics.uu.se

1 Department of Physics and Astronomy, Uppsala University, Uppsala, Sweden

2 Institute of Solid State Physics, TU Wien, Wien, Austria

References

[1]   Bogani L, Wernsdorfer W. Molecular spintronics using single-molecule magnets. Nature Materials. 2008;**7**:179

[2]   Wende H, et al. Substrate induced magnetic ordering and switching of iron porphyrin molecules. Nature Material. 2007;**6**:516

[3]   Bhandary S, Brena B, Panchmatia PM, Brumboiu I, Bernien M, Weis C, Krumme B, Etz C, Kuch W, Wende H, Eriksson O, Sanyal B. Manipulation of spin state of iron porphyrin by chemisorption on magnetic substrates. Physical Review B. 2013;**88**:024401

[4]   Bhandary S, et al. Correlated electron behavior of metal-organic molecules: Insights from density functional theory combined with many body effects using exact diagonalization. Physical Review B. 2016;**93**:155158

[5]   Gottfried JM. Surface chemistry of porphyrins and phthalocyanines. Surface Science Reports. 2015;**70**:259

[6]   Bhandary S et al. Graphene as a reversible spin manipulator of molecular magnets. Physical Review Letter. 2011;**107**:257202

[7] Geim AK. Graphene: Status and prospects. Science. 2009;**324**:1530

[8] Banhart F, Kotakoski J, Krasheninnikov AV. Structural defects in graphene. ACS Nano. 2011;**5**:26

[9] Liao M, Scheiner S. Electronic structure and bonding in metal porphyrins, metal = Fe, Co, Ni, Cu, Zn. Journal of Chemical Physics. 2002;**116**:205

[10] Klar D, Brena B, Herper HC, Bhandary S, Weis C, Krumme B, Schmitz-Antoniak C, Sanyal B, Eriksson O, Wende H. Oxygen-tuned magnetic coupling of Fe-phthalocyanine molecules to ferromagnetic Co films. Physical Review B. 2013;**88**:224424

[11] Herper HC, Bhandary S, Eriksson O, Sanyal B, Brena B. Fe phthalocyanine on Co(001): Influence of surface oxidation on structural and electronic properties. Physical Review B. 2014;**89**:085411

[12] Bhandary S, Eriksson O, Sanyal B. Defect controlled magnetism in FeP/graphene/Ni(111). Scientific Reports. 2013;**3**:3405

[13] Herper HC, Bernien M, Bhandary S, et al. Iron porphyrin molecules on Cu(001): Influence of adlayers and ligands on the magnetic properties. Physical Review B. 2013;**87**:174425

[14] Brena B, Herper HC. Influence of ligands on the electronic and magnetic properties of Fe porphyrin in gas phase and on Cu(001). JAP. 2015;**117**:17B318

[15] Stepanow S, Mugarza A, Ceballos G, Moras P, Cezar JC, Carbone C, Gambardell P. Giant spin and orbital moment anisotropies of a Cu-phthalocyanine monolayer. Physical Review B. 2010;**82**:014405

[16] Oguchi T, Shishidou T. Anisotropic property of magnetic dipole in bulk, surface, and overlayer systems. Physical Review B. 2004;**70**:024412

[17] Šipr O, Minár J, Ebert H. On the importance of the magnetic dipole term T_z in analyzing X-ray magnetic circular dichroism spectra of clusters. Europhysics Letter. 2009;**87**:67007

[18] van der Laan G. Relation between the angular dependence of magnetic x-ray dichroism and anisotropic ground-state moments. Physical Review B. 1998;**57**:5250

[19] Klar D, Bhandary S, et al. Field-regulated switching of the magnetization of Co-porphyrin on graphene. Physical Review B. 2014;**89**:144411